

Crystallization of the NADP-dependent  $\beta$ -keto acyl-carrier protein reductase from *Brassica napus*

Martin Fisher,<sup>a</sup> Svetlana E. Sedelnikova,<sup>a</sup> Wayne Martindale,<sup>b</sup> Neil C. Thomas,<sup>b</sup> J. William Simon,<sup>b</sup> Antoni R. Slabas<sup>b</sup> and John B. Rafferty<sup>a\*</sup>

<sup>a</sup>Krebs Institute for Biomolecular Research, Department of Molecular Biology and Biotechnology, The University of Sheffield, Sheffield S10 2TN, England, and <sup>b</sup>Lipid Molecular Biology Group, Department of Biological Sciences, The University of Durham, Durham DH1 3LE, England

Correspondence e-mail:  
j.rafferty@sheffield.ac.uk

Received 19 July 1999

Accepted 28 October 1999

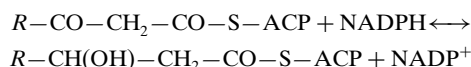
The NADP-dependent  $\beta$ -keto acyl-carrier protein reductase (BKR) from *Brassica napus* has been crystallized by the hanging-drop vapour-diffusion method using polyethylene glycol of average molecular weight 1500 as the precipitant. The crystals belong to the hexagonal space group  $P6_422$ , with unit-cell parameters  $a = b = 129.9$ ,  $c = 93.1$  Å,  $\alpha = \beta = 90^\circ$ ,  $\gamma = 120^\circ$ . Calculated values for  $V_m$ , the use of rotation and translation functions and consideration of the packing suggest that the asymmetric unit contains a monomer. The crystals diffract to beyond 2.8 Å resolution and are more amenable to X-ray diffraction analysis than those reported previously for the *Escherichia coli* enzyme. The structure determination of *B. napus* BKR will provide important insights into the catalytic mechanism of the enzyme and into the evolution of the fatty-acid elongation cycle by comparisons with the other oxidoreductase of the pathway, enoyl acyl-carrier protein reductase (ENR).

## 1. Introduction

Fatty-acid biosynthesis is critical for several essential cellular functions. These include membrane biogenesis, cell signalling and energy storage through the formation of triglycerides (Slabas & Fawcett, 1992). The *de novo* biosynthesis of fatty acids is catalyzed by fatty-acid synthetase (FAS) and involves elongation of a fatty-acid chain through the reiterative use of four enzymes at each cycle of elongation. Each cycle results in the incorporation of a two-carbon unit from malonyl acyl-carrier protein (ACP) and the loss of a molecule of carbon dioxide. The enzymes catalyze sequentially a condensation, a reduction, a dehydration and a final reduction (Slabas & Fawcett, 1992). Two types of FAS exist. Type I has the enzymes which catalyze individual steps in the pathway, with the associated ACP, on one or two multifunctional polypeptide chains, whereas type II has each catalytic domain individually located on separate polypeptide chains (Rock & Cronan, 1996). Plants and many bacteria contain the type II FAS.

The first reductive step of the FAS pathway catalyzes the reduction of the keto group of a  $\beta$ -ketoacyl ACP substrate to its hydroxy product and is catalysed by the NADP(H)-dependent enzyme  $\beta$ -keto acyl-carrier protein reductase (BKR; Sheldon *et al.*, 1992). It catalyzes the reversible reduction of 3-oxoacyl ACP to the D-(–)- $\beta$ -hydroxyacyl ACP isomer; the L-isomer is completely inactive as a substrate (Shimakata & Stumpf, 1982). The enzyme has a strong preference for the aceto-

acetyl ester of ACP over model substrates such as cysteamine or CoA derivatives (Sheldon *et al.*, 1992).



In plants, the enzyme has been successfully isolated from spinach leaves (Shimakata & Stumpf, 1982), avocado mesocarp (Sheldon *et al.*, 1990) and oilseed rape (Sheldon *et al.*, 1992). The monomer of BKR from *B. napus* has an  $M_r$  of approximately 28 kDa as determined from the amino-acid sequence derived from the cDNA (Slabas *et al.*, 1992) and is composed of 260 amino acids. Gel-filtration studies on the enzyme are consistent with it being a tetramer in spinach (Shimakata & Stumpf, 1982), oilseed rape (Sheldon *et al.*, 1992) and avocado (Sheldon *et al.*, 1990).

Sequence analysis has shown a high degree of similarity (34% completely conserved with respect to the *B. napus* sequence) between the known BKR enzymes from a range of species (Slabas *et al.*, 1992) and provides an initial indication that the overall structure of BKR from plants and bacteria will be very similar and that this similarity might extend to the details of the catalytic mechanism. Further sequence analysis has also suggested that BKR belongs to a short-chain alcohol dehydrogenase (SDR) family for which the structures of a number of members have been determined, including that of 3 $\alpha$ ,20 $\beta$ -hydroxysteroid dehydrogenase (HSD) from *Streptomyces hydrogenans* (Ghosh *et al.*, 1994). The SDR family members possess a char-

acteristic sequence motif formed by a triad of conserved serine, tyrosine and lysine residues involved in the catalytic mechanisms of the enzymes of the family (Jörnvall *et al.*, 1995).

BKR has also been noted to possess 25% sequence identity to enoyl reductase (ENR), the second reductive enzyme of the fatty-acid elongation cycle, hence prompting the suggestion of an evolutionary relationship (Rafferty *et al.*, 1995). Although both enzymes carry out reductive steps in fatty-

acid biosynthesis, they reduce quite different targets, with BKR reducing a carbon-oxygen double bond whereas ENR reduces a carbon-carbon double bond. The structure of the ENR from *B. napus* has been determined (Rafferty *et al.*, 1995), thus making possible a comparison with BKR and examination of the molecular differences underlying the two reductive processes. Solving the structure of the *B. napus* BKR should give a greater understanding of the mechanism and substrate binding of the BKR family than is currently available and should provide an opportunity to study the evolutionary relationship to *B. napus* ENR.

## 2. Experimental

$\beta$ -Keto reductase from *B. napus* was purified from an over-expressing *E. coli* strain BL21(DE3) which had previously been transformed with the pETJRS10.1 plasmid, a construct of pET11d containing the cloned *B. napus* mature protein sequence. PCR primers had been designed to enable insertion and ligation of the mature coding sequence for the *B. napus* BKR cDNA (Slabas *et al.*, 1992). Cells were grown at 310 K with ampicillin selection in LB medium, induced with 100  $\mu$ M IPTG and then

harvested by centrifugation and frozen. All subsequent steps were carried out at 277 K.

The cells were resuspended in 40 mM Tris-HCl pH 8, 2 mM EDTA (buffer A) and cell disruption was achieved by sonication at  $4 \times 20$  s in a Soniprep-200 sonicator with amplitude 16–18  $\mu$ m. Debris was removed by centrifugation at 25 000g for 15 min. The resulting crude cell extract showed a high level of BKR activity in an optical assay employing the substrate analogue acetoacetyl-CoA (Sheldon *et al.*, 1990). The supernatant was treated with protamine sulfate at a concentration of 5 mg ml<sup>-1</sup> of crude extract and centrifuged at 25 000g for 10 min. The supernatant was then loaded onto a DEAE-Sephacose column equilibrated in buffer A. BKR did not bind to this column but many contaminants were removed, increasing the protein purity. 4 M ammonium sulfate was added to the protein sample until a concentration of 1.5 M was reached; it was then re-centrifuged at 25 000g for 10 min. The supernatant was then loaded onto a butyl-Toyopearl 650s column equilibrated with 1.5 M ammonium sulfate in buffer A and eluted with 1.3 M ammonium sulfate. A sample of protein was run on an SDS-PAGE gel and the purity of BKR was calculated to be approximately 60–70%. The purified sample was concentrated using a VIVASPIN 15 (30 kDa molecular-weight cutoff PED membrane) concentrator (Vivascience Ltd, UK) to a concentration of  $\sim 7$ –10 mg ml<sup>-1</sup> and dialysed in 10 mM Tris-HCl pH 8 overnight. Precipitated contaminants were removed by centrifugation at 28 000g for 5 min. The final BKR enzyme preparation was approximately 80% pure as estimated by SDS-PAGE.

### 2.1. Crystallization

For the crystallization trials, BKR protein samples were dialysed against 50 mM sodium phosphate pH 6.0, 1 mM DTT. Samples of the protein were mixed prior to crystallization trials with NADP<sup>+</sup> to give a final NADP<sup>+</sup> concentration of 5 mM. Small volumes (5–10  $\mu$ l) of the protein plus cofactor samples were mixed with an equal volume of a precipitant solution of polyethylene glycol average molecular weight 1500 over the concentration range 8–12% (w/v) in 100 mM sodium citrate buffer pH 4.0 and were allowed to equilibrate by vapour diffusion with reservoirs of precipitant solution at 290 K. Crystals with a hexagonal bipyramidal morphology and maximum dimensions of  $0.25 \times 0.40 \times$

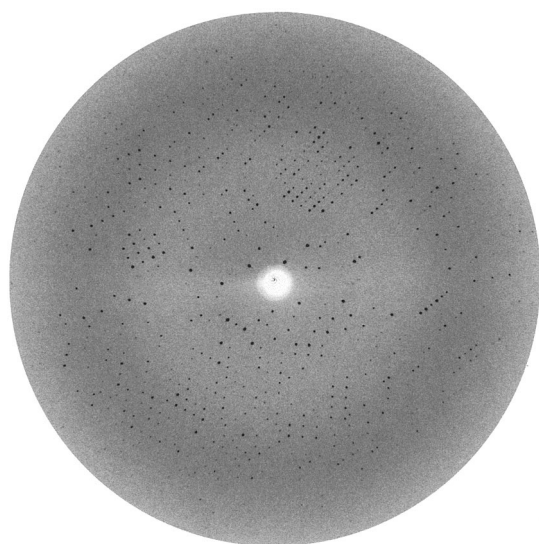


**Figure 1**

An X-ray diffraction image recorded at room temperature on a large MAR Research image plate on station 9.5 at the CLRC Daresbury SRS. The diffraction limit to the edge of the image is 2.8 Å and a rotation angle of 2° was used.

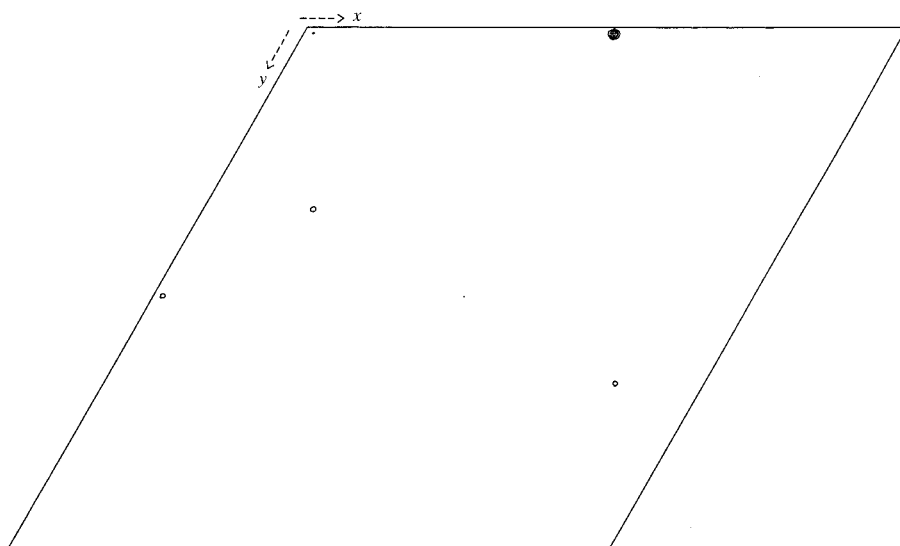


**Figure 2**

A section from the translation function for BKR obtained using a monomer of HSD as a search model in space group *P*6<sub>3</sub>22. The section (at 0.488 of the cell on *Z* and showing the whole cell in *X* and *Y*) shows the major peak in the map which gave a clear solution (18 $\sigma$ ) consistent with packing considerations.

0.25 mm were obtained after approximately one week.

## 3. Results and discussion

A diffraction data set was collected at room temperature by the rotation method with 2° rotations per frame at an X-ray wavelength of 1.1 Å on station 9.5 at the CLRC Synchrotron Source, Daresbury, using a large MAR Research image plate (Fig. 1). The crystals contain a hexagonal lattice and diffract to better than 2.8 Å resolution. Accurate unit-cell parameters were determined to be  $a = b = 129.9$ ,  $c = 93.1$  Å,  $\alpha = \beta = 90$ ,  $\gamma = 120^\circ$ , with a resultant unit-cell volume of  $1.36 \times 10^6$  Å<sup>3</sup>. Data were processed and analysed using the *HKL* suite of programs (Otwinowski & Minor, 1997) and the *CCP4* suite of programs (Collaborative Computational Project, Number 4, 1994) in space group *P6* and gave a data set 79.0% complete to 2.8 Å resolution, with 25 934 measurements of 17 685 unique reflections with an overall multiplicity of 1.5 and a merging *R* factor of 7.5%. A view of the *hk0* plane using the program *HKLVIEW* (Collaborative Computational Project, Number 4, 1994) indicated the presence of additional twofold axes and suggested the space group could be a derivative of point group *P622*. This analysis implied that there was a monomer in the asymmetric unit, giving a value for the  $V_m$  of 4.05 Å<sup>3</sup> Da<sup>-1</sup> and a solvent content of 70%, which lies on the high side of the normal range for proteins (Matthews, 1977). The data were reprocessed in space group *P622* and gave a data set 89.3% complete to 2.8 Å resolution with 25 915 measurements of 10 096 unique

reflections with an overall multiplicity of 2.6 and a merging *R* factor of 8.5% [with a merging *R* factor of 32%, a multiplicity of 2.4 and an  $I/\sigma(I)$  of 2.1 in the highest resolution shell, 2.87–2.80 Å]. The morphology and fragility of the crystals made attempts to obtain measurements of reflections along the sixfold axis difficult and thus it was not possible to determine whether a screw axis was present simply by looking for patterns of systematic absences. An attempt was made to determine a molecular-replacement solution for BKR using the known structure of HSD as a search model. A cross rotation function for the tetramer was calculated on data from 8–3.5 Å resolution with a 25 Å radius of integration using the program *POLARRFN* (Kabsch, unpublished work; Collaborative Computational Project, Number 4, 1994). A clear solution was obtained and a translation function was calculated for all space groups derived from point group *P622* using the program *TFEC* (Collaborative Computational Project Number 4, 1994). A unique solution was obtained with a signal-to-noise ratio of over 18σ (the root-mean-square deviation from mean density on the map) for space group *P6<sub>4</sub>22*, with the second peak having a signal-to-noise ratio of 4.5σ (Fig. 2). The packing was checked using the program *FRODO* (Jones, 1978).

Attempts to refine the structure based upon the molecular-replacement solution phases are currently under way.

We thank the support staff at the CLRC Synchrotron Radiation Source at Daresbury for assistance with station alignment. This

work was supported by grants from the BBSRC to JBR and ARS. JBR is a BBSRC David Phillips Fellow. MF is a NEDO funded researcher. The Krebs Institute is a designated BBSRC Biomolecular Science Centre and a member of the North of England Structural Biology Centre.

## References

- Collaborative Computational Project, Number 4 (1994). *Acta Cryst.* **D50**, 760–763.
- Ghosh, D., Wawrzak, Z., Weeks, C. M., Duax, W. L. & Erman, M. (1994). *Structure*, **2**, 629–640.
- Jones, T. A. (1978). *J. Appl. Cryst.* **11**, 118–147.
- Jörnvall, H., Persson, B., Krook, M., Atrian, S., Gonzalez-Duarte, J. J. & Ghosh, D. (1995). *Biochemistry*, **34**, 6003–6013.
- Matthews, B. W. (1977). *The Proteins*, 3rd ed., Vol. 3, edited by H. Neurath & R. L. Hill, pp. 468–477. New York: Academic Press.
- Otwinowski, Z. & Minor, W. (1997). *Methods Enzymol.* **276**, 307–326.
- Rafferty, J. B., Simon, J. W., Baldock, C., Artymiuk, P. J., Baker, P. J., Stuitje, A. R., Slabas, A. R. & Rice, D. W. (1995). *Structure*, **3**, 927–938.
- Rock, C. O. & Cronan, J. E. (1996). *Biochim. Biophys. Acta*, **1302**, 1–16.
- Sheldon, P. S., Kekwick, R. G. O., Sidebottom, C., Smith, C. G. & Slabas, A. R. (1990). *Biochem. J.* **271**, 713–720.
- Sheldon, P. S., Kekwick, R. G. O., Smith, C. G., Sidebottom, C. & Slabas, A. R. (1992). *Biochim. Biophys. Acta*, **1120**, 151–159.
- Shimakata, T. & Stumpf, P. K. (1982). *Arch. Biochem. Biophys.* **218**, 77–91.
- Slabas, A. R., Chase, D., Nishida, I., Murata, N., Sidebottom, C., Safford, R., Sheldon, P. S., Kekwick, R. G. O., Hardie, D. G. & Mackintosh, R. W. (1992). *Biochem. J.* **283**, 321–326.
- Slabas, A. R. & Fawcett, T. (1992). *Plant Mol. Biol.* **19**, 169–191.